ROYAL SOCIETY OF CHEMISTRY

PAPER

Synthesis and structural investigation of a series of mannose-containing oligosaccharides using mass spectrometry†

S. Daikoku,‡[a] R. Pendrill,‡[b] Y. Kanie, [ID][a] Y. Ito, [ID][c] G. Widmalm [ID] *[b] and O. Kanie [ID] *[a]

A series of compounds associated with naturally occurring and biologically relevant glycans consisting of α-mannosides were prepared and analyzed using collision-induced dissociation (CID), energy-resolved mass spectrometry (ERMS), and ^{1}H nuclear magnetic resonance spectroscopy. The CID experiments of sodiated species of disaccharides and ERMS experiments revealed that the order of stability of mannosyl linkages was as follows: 6-linked > 4-linked ≧ 2-linked > 3-linked mannosyl residues. Analysis of linear trisaccharides revealed that the order observed in disaccharides could be applied to higher glycans. A branched trisaccharide showed a distinct dissociation pattern with two constituting disaccharide ions. The estimation of the content of this ion mixture was possible using the disaccharide spectra. The hydrolysis of mannose linkages at 3- and 6-positions in the branched trisaccharide revealed that the 3-linkage was cleaved twice as fast as the 6-linkage. It was observed that the solution-phase hydrolysis and gas-phase dissociation have similar energetics.

Introduction

In order to elucidate the glycan structure of naturally occurring oligosaccharide samples, the use of a logically arranged array of compounds as a data source is considered advantageous.[1–3] Although an array of compounds should provide a complete set of structural data, it is often very difficult to obtain such a library. A variety of *manno*-oligosaccharides exist in nature, some of which are shown in Fig. 1 with symbolic structures.[4–7] A mammalian high mannose-type *N*-linked glycan is composed of nine mannoses with different anomeric configurations and linkage positions, and it plays an important role in the folding of glycoproteins in endoplasmic reticulum and is later reconstructed into complex *N*-glycans in Golgi apparatus.[8–10] The hybrid type of *N*-linked glycan is associated with infectious diseases and immunity.[11–15] Other forms of mannose-containing oligosaccharides *i.e.*, glycosylphosphatidylinositol anchored glycoprotein,[16] and cell wall polysaccharides of *Saccharomyces cerevisiae*[17,18] and *Mycobacterium*

[a]*Department of Applied Biochemistry, Tokai University, 4-1-1 Kitakaname, Hiratsuka, Kanagawa 259-1292, Japan. E-mail: kanie@u-tokai.ac.jp*
[b]*Department of Organic Chemistry, Arrhenius Laboratory, Stockholm University, S-106 91 Stockholm, Sweden*
[c]*Synthetic Cellular Chemistry Laboratory, RIKEN, 2-1 Hirosawa, Wako, Saitama 351-0198, Japan*
†Electronic supplementary information (ESI) available. See DOI: 10.1039/c7ob02723k
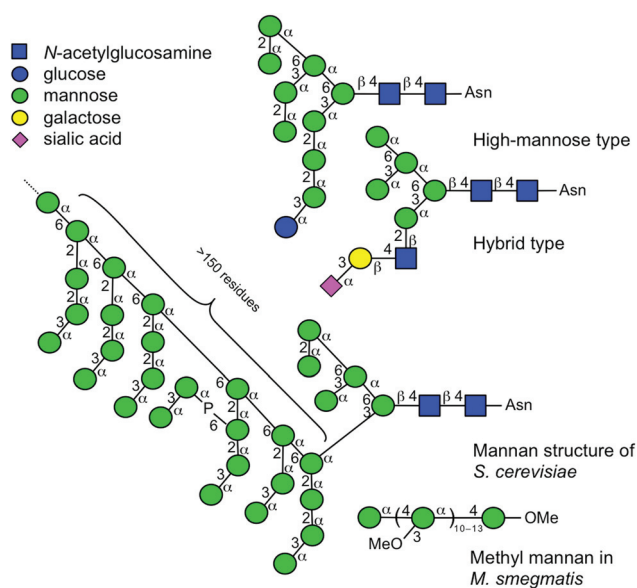‡These authors contributed equally.

Fig. 1 Symbolic representations of naturally occurring glycans consisting of multiple mannosyl residues. Symbols are used as suggested.[4–7] Individual linkage isomers are shown with distinctive angle presentations.[4]

smegmatis[19] also exist. Surprisingly, when considering α-linked mannosyl residues, all the possible linkage isomers, namely mannose (Man) residues linked to 2-, 3-, 4-, and 6-positions of adjacent Man, exist in nature.

228 | *Org. Biomol. Chem.*, 2018, **16**, 228–238

This journal is © The Royal Society of Chemistry 2018

Therefore, it is important to discriminate individual structures. As the amounts of samples obtainable from natural sources are often limited, mass spectral analysis is an excellent technique for structural investigations. In particular, low-energy collision-induced dissociation (CID) and ion mobility mass spectrometry are suitable techniques for the differentiation of subtle structural differences.[1,20,21]

Herein, we perform the mass spectrometric analysis of synthetic compounds useful for investigating larger oligosaccharide structures. A series of disaccharides and trisaccharides, namely, αMan–(1 → 2)–αMan–OMe (**1**), αMan–(1 → 3)–αMan–OMe (**2**), αMan–(1 → 4)–αMan–OMe (**3**), αMan–(1 → 6)–αMan–OMe (**4**), αMan–(1 → 2)–αMan–(1 → 2)–αMan–OMe (**5**), αMan–(1 → 2)–αMan–(1 → 3)–αMan–OMe (**6**), αMan–(1 → 2)–αMan–(1 → 6)–αMan–OMe (**7**), and αMan–(1 → 3)–[αMan–(1 → 6)–]αMan–OMe (**8**) individually representing partial structures of biologically relevant glycan structures (Fig. 2) were analyzed.
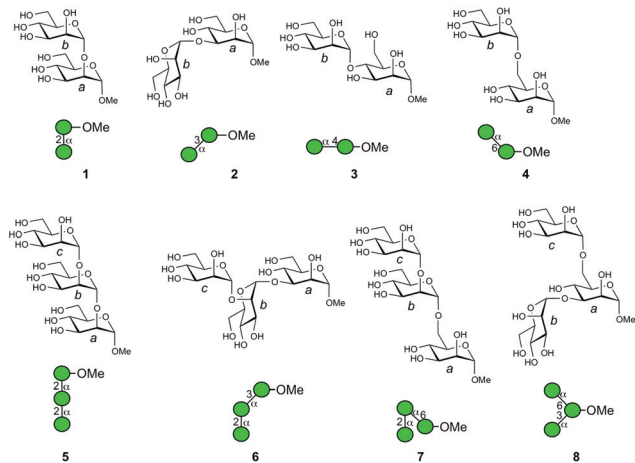

Fig. 2 Structures of oligomannosides investigated. The individual mannose residues are designated as *a*, *b*, and *c* by reducing the end terminus for clarity in the molecular structures. Symbolic representations of the structures are also provided.

The results provide valuable information about the order of stability of mannosyl linkages, and the fragmentation analyses of individual ions with different linkages were carried out in detail. We also showed that the analysis of a mixture of ions obtained from a branched structure is possible. A comparison of the gas-phase CID reaction and acid hydrolysis reaction in solution was also carried out.

Results and discussion

Oligosaccharide synthesis

The chemical synthesis of D-mannosyl-containing α-(1 → 4)-linked disaccharide **3** and αMan–(1 → 2)–αMan–(1 → 6)-linked trisaccharide **7** and its [6-¹³C]-isotopologue **7c** was carried out *via* N-iodosuccinimide/silver triflate promoted glycosylation as the key reaction (Scheme 1). The coupling of donor **10** with acceptor **9** in the temperature interval of −50 °C to −30 °C proceeded smoothly to result in the anticipated α-(1 → 4)-linked disaccharide **11** in good yield (84%).

The subsequent two-step deprotection procedure employing hydrogenolysis first with palladium hydroxide on carbon as the catalyst followed by O-debenzoylation under Zemplén conditions resulted in target disaccharide **3** in 55% yield over two steps. In the synthesis of trisaccharide **7**, the O-benzylated acceptor **12** was glycosylated by the suitably protected mannosyl donor **13** with an acetyl group installed at O2, thereby facilitating neighboring group participation ensuring that an α-linkage was formed in the disaccharide product; this was followed by the removal of the O-acetyl group using sodium methoxide in methanol, thereby unmasking the alcohol function to result in **14** in 53% yield over two steps. Disaccharide **14** was subsequently coupled with donor **10** under the same experimental conditions as in the previous glycosylation step, which subsequently resulted in trisaccharide **15** in 67% yield. Employing the same two-step deprotection procedure for the above disaccharide resulted in trisaccharide **7**, albeit with 31%
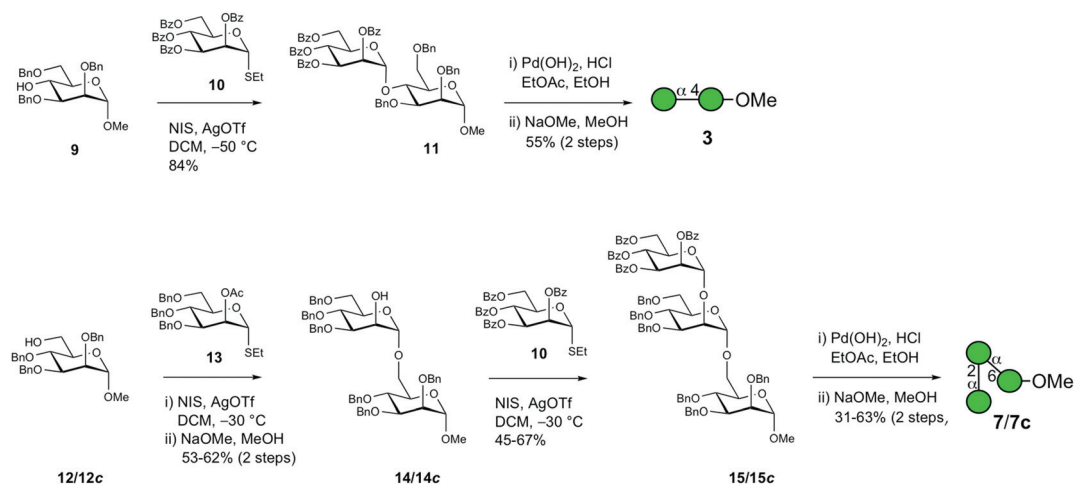
Scheme 1 Synthesis of oligosaccharides **3**, **7** and **7c**.

yield. Synthesis of the corresponding 4-aminophenyl glycoside of **7** was previously described by Khan *et al.*[22] The ^{13}C-isotopologue **7c**, which has been investigated using nuclear magnetic resonance (NMR) relaxation experiments,[23] was synthesized using the same protocol; the yields of the first glycosylation reaction and deprotection steps were, in this case, improved to 62% and 63%, respectively.

Structural details of disaccharides obtained from low-energy CID experiments

In order to understand the structural details of a series of oligosaccharides, the analysis of the fragmentation process of the corresponding precursor ions was carried out. Prior to the investigation, we decided to analyze sodium adducted molecules in the CID experiments, because they are frequently observed without any preparative manipulation and they provide data superior to those of proton adducts in energy-resolved mass spectrometry (ERMS).[24,25] The common ions produced during the CID process of the sodiated precursor ions obtained for compounds **1–4** are ions with m/z 185 (B_1) and 217 (Y_1), each corresponding to the units *b* and *a*. (Fig. 3) (Assignment of ion species was done according to Domon and Costello.[26]) A pair of ions with m/z 185 and 217 correspond to the cleavage of a glycosidic bond at the non-reducing end of the mannosyl residue. As these ions are common in all disaccharides, the m/z values themselves cannot be used to

diagnose the structures. However, the ratio of these cleavages can be used for the verification, called a "spectral matching technique."[27,28] The percentages of these glycosyl cleavages are shown in the table in Fig. 3. As evident from the table, these cleavage reactions are the major process in each case. A characteristic feature is the preferential methyl glycoside cleavage in sodiated compound **2**. A clear explanation cannot be provided for this phenomenon but this can be a diagnostic event. Compounds **3** and **4** in their sodiated forms provided a similar fragmentation pattern with a preferential formation of the X-ion series. In these fragmentation reactions, the $^{3,5}X_1$ ion (m/z = 319) was formed in the spectrum for **3**, and $^{0,2}X_1$ ion (m/z = 245) and $^{0,3}X_1$ ion (m/z = 275) were characteristic of **4**. We also investigated the fragmentation of sodiated isotopologue **4c** [**4c** + Na^{+}], in which C6 of the reducing terminus mannoside was replaced with [13]C. A series of product ions produced during the CID of the sodiated compound was observed to be virtually identical to that of parent **4**. This type of evidence might be useful in the investigation of pulse-chase experiments.[29] Although cross-ring cleavages are useful in identifying linkage isomers, an ion with m/z = 319 which could be assigned to be the $^{2,4}X_1$ ion might be used to identify 4-linked mannoside only.

We subsequently analyzed the energy dependence of the fragmentation reactions of individual sodiated disaccharides. We focus on the decay process of precursor ions during ERMS
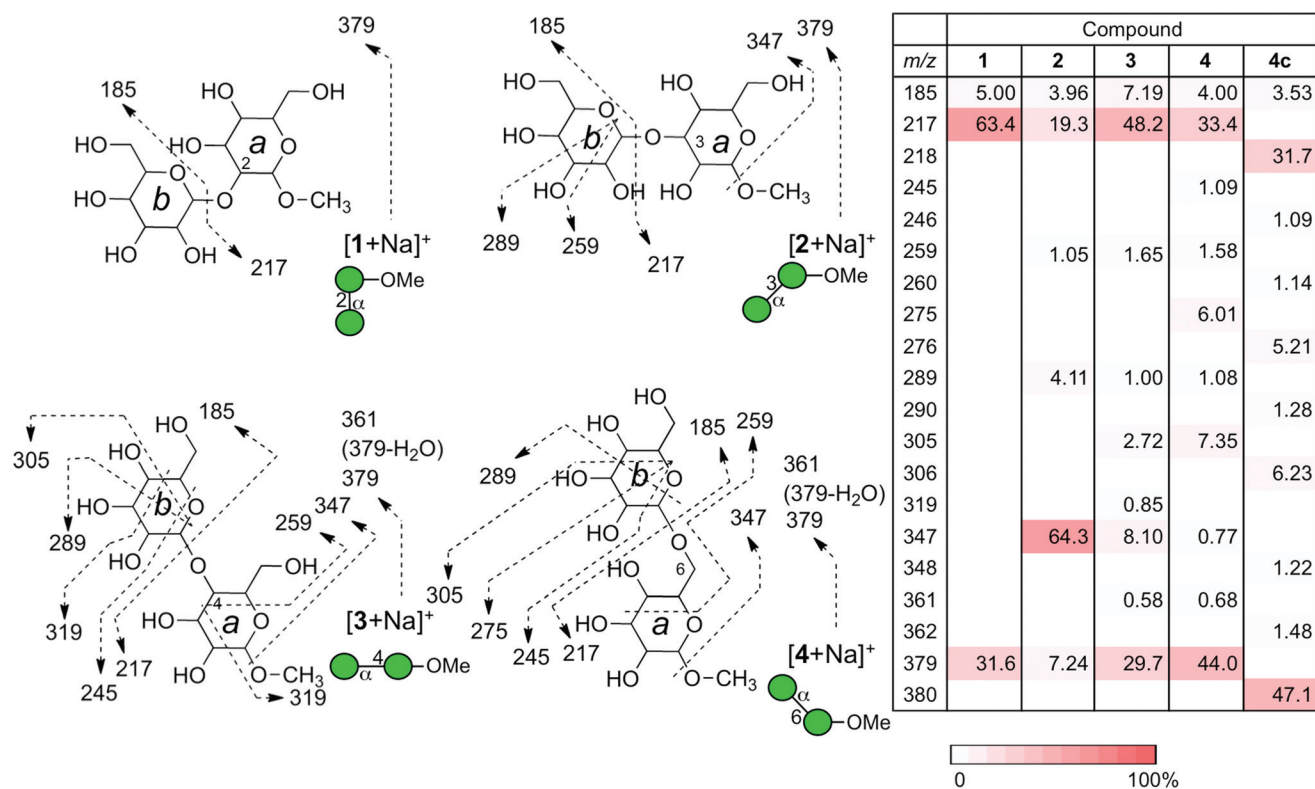

m/z	Compound				
	1	2	3	4	4c
185	5.00	3.96	7.19	4.00	3.53
217	63.4	19.3	48.2	33.4	
218					31.7
245			1.09		
246					1.09
259		1.05	1.65	1.58	
260					1.14
275				6.01	
276					5.21
289		4.11	1.00	1.08	
290					1.28
305			2.72	7.35	
306					6.23
319			0.85		
347		64.3	8.10	0.77	
348					1.22
361			0.58	0.68	
362					1.48
379	31.6	7.24	29.7	44.0	
380					47.1

0   100%

Fig. 3 Fragmentation patterns of a series of sodiated disaccharides under CID conditions. The observed fragments are indicated in structures. The CID experiments were conducted at the end-cap radio frequency amplitude of 0.7 V. The table summarizes the intensities of individual product ions. The relative ion intensities are indicated by a red-colored scale.
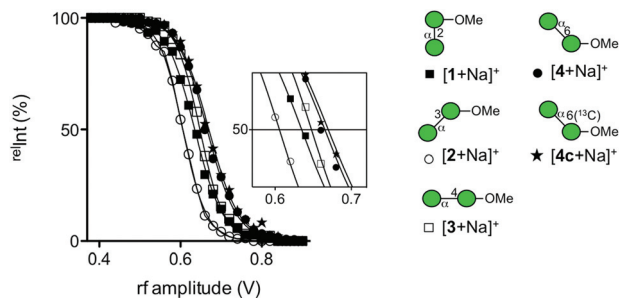
230 | *Org. Biomol. Chem.*, 2018, **16**, 228–238

This journal is © The Royal Society of Chemistry 2018

Fig. 4 Decay curves of a series of sodiated disaccharides obtained *via* ERMS experiments. $[1 + Na]^+$ (■), $[2 + Na]^+$ (○), $[3 + Na]^+$ (□), $[4 + Na]^+$ (●), and $[4c + Na]^+$ (★).

(Fig. 4). The decay curves indicate the conversion process of individual precursor ions into product ions under CID conditions, which cannot be obtained *via* standard MS/MS experiments. The most labile disaccharide appeared to be the 3-linked compound **2** whereas 6-linked **4** was the most stable. The difference observed between sodiated **4** and its ^{13}C-labeled counterpart **4c** is believed to reflect the mass difference in the dissociation reaction. The decay curves of 2- (**1**) and 4-linked (**3**) disaccharides were in between these two disaccharides and showed similar reactivities under the given conditions. A visual inspection of the decay process of individual precursor ions in ERMS indicated the order of stability to be: 6-linked > 4-linked ≥ 2-linked > 3-linked disaccharide. It has been reported that the primary glycosidic linkage is stable, which

can be explained by the rotational freedom around the glycosidic linkage compared to the secondary linkages.[2]

Dissociation of a series of sodiated linear trisaccharides: *c–b–a*–OMe

A series of linear trisaccharides individually consisting of three distinct glycosidic linkages were subsequently analyzed. At a glance, dehydration ions with $m/z = 523$ ($[M + Na-H_2O]^+$) observed for **5** only, [3,5]A_3 ions with $m/z = 451$ for **6** and [1,5]X_2 ions with $m/z = 467$ for **7** are characteristic of the linkage isomers in the *b–a* units. Among a variety of product ions formed during the CID process, the major cleavage pathway in all the cases was the glycosyl rupture (Fig. 5). However, the intensities of signals corresponding to individual glycosyl cleavages were different.

The sums of intensities for the glycosyl cleavages between units *b* and *c* (intensity (Int.) for $[c + Na]^+$ + Int. $[(b–a) + Na]^+$) were 55.4% for αMan–(1 → 2)–αMan–(1 → 2)–αMan–OMe (**5**), 39.4% for αMan–(1 → 2)–αMan–(1 → 3)–αMan–OMe (**6**), and 72.9% for αMan–(1 → 2)–αMan–(1 → 6)–αMan–OMe (**7**). The intensities of signals for the cleavage between units *a* and *b* (Int. m/z 217 + Int. m/z 347 + Int. m/z 329) were 35.9% (**5**), 24.6% (**6**), and 11.4% (**7**). The intensities associated with the dissociation of the methyl group were zero (not observed) (**5**), 28.1% (**6**), and 1.78% (**7**). Interestingly, the tendency of reducing the methyl glycoside cleavage in the ion of (**6**) can be observed in the CID data for one of the disaccharides, namely αMan–
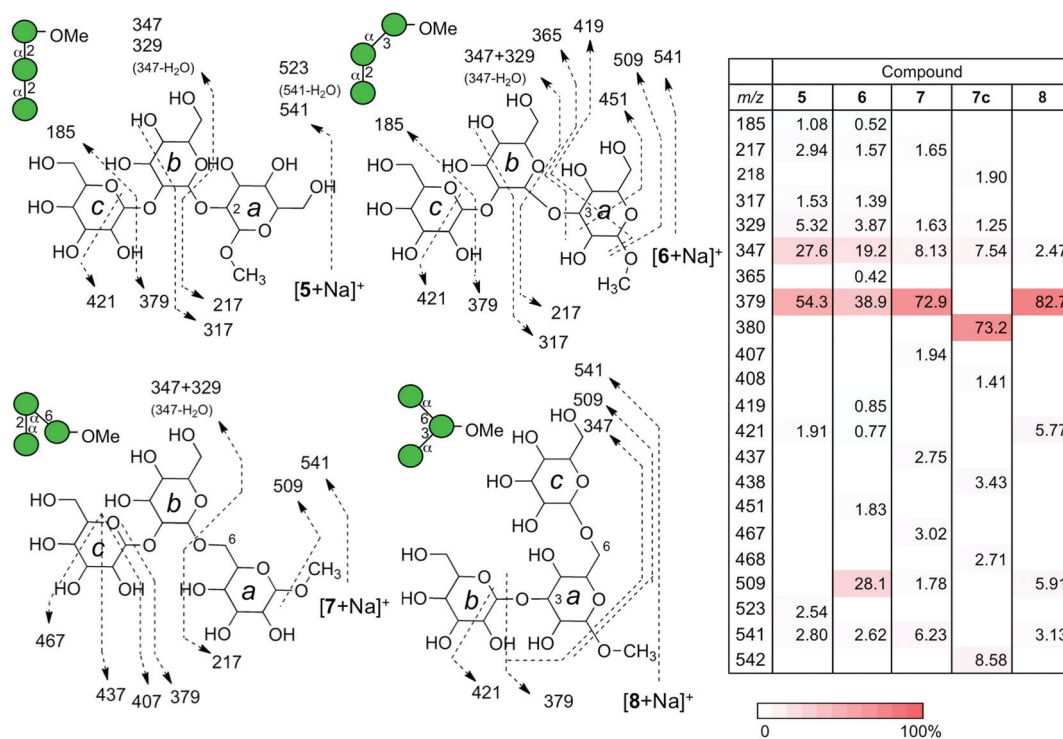

Fig. 5 Fragmentation patterns of a series of sodiated trisaccharides under CID conditions. The CID experiments were conducted at the end-cap radio frequency amplitude of 0.7 V. The table summarizes the intensities of individual product ions. A designated red intensity scale is also shown.

m/z	Compound				
	5	**6**	**7**	**7c**	**8**
185	1.08	0.52			
217	2.94	1.57	1.65		
218				1.90	
317	1.53	1.39			
329	5.32	3.87	1.63	1.25	
347	27.6	19.2	8.13	7.54	2.47
365		0.42			
379	54.3	38.9	72.9		82.7
380				73.2	
407			1.94		
408				1.41	
419		0.85			
421	1.91	0.77			5.77
437			2.75		
438				3.43	
451		1.83			
467			3.02		
468				2.71	
509		28.1	1.78		5.91
523	2.54				
541	2.80	2.62	6.23		3.13
542				8.58	

This journal is © The Royal Society of Chemistry 2018

Org. Biomol. Chem., 2018, **16**, 228–238 | **231**

$(1 \rightarrow 3)$–αMan–OMe (**2**), which shares the same 3-linked disaccharide structure.

Since the energy dependence of individual ions is quite complex and reflects various factors, we attempted to consider the internal energy as a reference point. The order of ion stability of a series of sodiated disaccharides observed under the CID conditions was as follows: 6-linked > 4-linked ≥ 2-linked > 3-linked, as described above. It is difficult to discuss the underlying mechanism using the data alone. However, as a series of linear trisaccharides contained the same disaccharide structure, we surmised that it would be possible to determine a correlation between the structure and the observed order of ion stability. Thus, the non-reducing mannosyl residue (unit *c*) is considered to be an internal energy reference because the position and anomeric configuration of the residue are the same and furthermore, the structural similarity makes it suitable to evaluate other inter-mannosyl linkages between units *a* and *b*. Although methyl glycoside was common to all the compounds, it was not considered to be appropriate as an internal energy reference because the residue was closely associated with the cleavage of linkage *a*–*b*.

Thus, we compared the sum of intensities of signals associated with individual glycosyl cleavages and obtained a ratio *a*–*b*/*b*–*c* to compare the relative strength of mannosyl linkages present in a structure. The obtained *a*–*b*/*b*–*c* values were 0.55 (**5**), 0.56 (**6**), and 0.10 (**7**). This indicates that the stability order is 6-linked > 2-linked ≥ 3-linked, which is consistent with the order observed for the stability of disaccharides. Moreover, the CID of an isotope labeled compound **7c**, at C6 of reducing terminus mannoside, resulted in an almost identical fragmentation pattern with one atom unit shifts in the product ions carrying ^{13}C instead of ^{12}C.

Dissociation of the branched trisaccharide: *b*–(*c*–)*a*–OMe

Naturally occurring manno-oligosaccharides often contain a branching structure with $\alpha(1 \rightarrow 3)$- and $\alpha(1 \rightarrow 6)$-linkages (Fig. 1). Therefore, compound **8** would serve as a valuable information source. The CID analysis of sodiated αMan–$(1 \rightarrow 3)$–[αMan–$(1 \rightarrow 6)$–]αMan–OMe (**8**) was carried out (Fig. 5). The fragmentation pattern resembled that of sodiated **7** having a 6-linkage, rather than that of **6** having a 3-linkage, observed with an ion at *m/z* 379 corresponding to the Y-ion structure (*b*–*a* unit) that lost a non-reducing mannosyl residue (*c* unit) resulting in a prominent product ion. This indicates that the relative strengths of glycosidic linkages at the 3- and 6-positions are quite different, as clearly shown in the dissociation of disaccharides, where 6-linked mannose is more stable (Fig. 4). Therefore, the glycosyl cleavage at the 3-position will predominantly occur in sodiated **8**.

MS/MS results of a series of product ions with *m/z* 379 produced from sodiated trisaccharides

The CID experiments of sodiated disaccharide ions for unit *b*–*a* (*m/z* 379) produced from a series of sodiated trisaccharides were carried out at the MS^3 stage to investigate whether the product ions are identical to the fragmentation patterns of
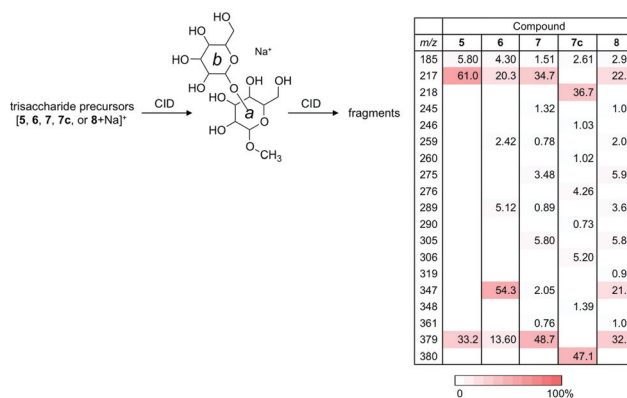

m/z	Compound				
	5	6	7	7c	8
185	5.80	4.30	1.51	2.61	2.98
217	61.0	20.3	34.7		22.7
218				36.7	
245			1.32		1.03
246				1.03	
259		2.42	0.78		2.09
260				1.02	
275			3.48		5.90
276				4.26	
289		5.12	0.89		3.69
290				0.73	
305			5.80		5.88
306				5.20	
319					0.91
347		54.3	2.05		21.3
348				1.39	
361			0.76		1.01
379	33.2	13.60	48.7		32.5
380				47.1	

0   100%

Fig. 6 MS^3 experiments of Y-ions produced from a series of sodiated trisaccharides under CID conditions. The series of product ions for individual precursors are virtually identical to those obtained from the corresponding disaccharide ions at MS^2.

those of the disaccharide library (Fig. 6). According to our previous results, the Y-ion species are treated as "pure" ions without any structurally isomeric ions, and thus can be used for the structural identification at different stages of MS^n.[25] Therefore, these types of ion species are suitable for structural identification. The fragmentation products and their intensities were strikingly similar to those of the corresponding disaccharides indicating that the structures of Y-ions produced from trisaccharides can be deduced from those of library disaccharides except for the branched compound. In the current experiment, using a library of disaccharides, the CID data were used to identify the partial structure of a trisaccharide. When we assume that the structure of a trisaccharide is not known, the partial structure $[b–a + Na]^+$ is determined at the MS^3 stage by comparing a series of data from a library.

Regarding the product ion obtained from the branched trisaccharide ion, the structure *b*–(*c*–)*a*-OMe (**8**) contains both 3- and 6-linked mannosyl residues. As mentioned above, the fragmentation pattern of the produced ion with *m/z* 379 was similar to that of $[2 + Na]^+$ with some minor ions observed in the fragmentation of $[4 + Na]^+$, indicating that the formed Y-ion may be a mixture of these two product ions.

We thus carried out an ERMS experiment on the produced Y-ion corresponding to the partial structure of trisaccharide **8**, and compared it with those of authentic disaccharides, namely **2** and **4**. As shown in Fig. 7, the decay curve obtained for the degradation of the Y-ion generated from $[8 + Na]^+$ was observed in between those of individual decay curves of $[2 + Na]^+$ and $[4 + Na]^+$. This suggested that the Y-ion was a mixture of these two ions, which is consistent with the result of MS/MS experiments.

We subsequently estimated the contents of $[2 + Na]^+$ and $[4 + Na]^+$ in the Y-ion mixture obtained from the branched trisaccharide $[8 + Na]^+$. Accordingly, the ion intensities of individual product ions at the resonant frequency amplitude of 0.7 V were used. Consequently, it was estimated that the Y-ion produced was a mixture of $[2 + Na]^+$ (37%) and $[4 + Na]^+$ (63%)

232 | *Org. Biomol. Chem.*, 2018, **16**, 228–238

This journal is © The Royal Society of Chemistry 2018

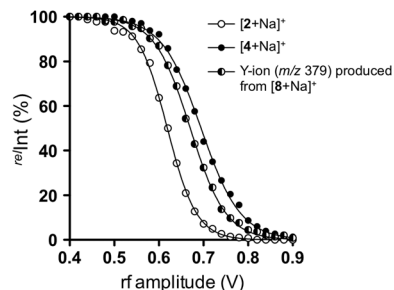**Fig. 7** Comparison of decay curves of sodiated disaccharides (**2** and **4**) and Y-ion obtained from sodiated **8** in ERMS. $[2 + Na]^+$ (○), $[4 + Na]^+$ (●), and Y-ion (m/z 379) produced by CID of $[8 + Na]^+$ (◑).

based on the assumption that there was no loss of ions during the CID (Fig. 8). Subtle differences could be observed in these spectra, which were attributed to the different populations of differently sodiated ion species (different coordination sites).

Oligosaccharide hydrolysis monitored using NMR

At this stage, we considered whether the gas phase CID reactions were related to the hydrolysis reactions. We performed acidic hydrolyses of compounds **2**, **4**, and **8** to examine the reactivities of 3- and 6-linked glycosidic bonds under ^{1}H NMR monitoring (Fig. 9a). In trisaccharide **8**, substitution by α-ᴅ-mannopyranosyl groups occurred at secondary and primary alcohol groups, *i.e.*, at *O*3 and *O*6, respectively. In order to study the relative stability to hydrolysis at these glycosidic linkages, the trisaccharide was subjected to acid hydrolysis at an elevated temperature (1 M trifluoroacetic acid, D₂O, 70 °C) and monitored using ^{1}H NMR spectroscopy. As a reference, both the α(1 → 3)- and α(1 → 6)-linked disaccharides **2** and **4**, respectively, were investigated under corresponding experimental conditions. The progress of the hydrolysis reaction was analyzed by monitoring the disappearance of the ^{1}H resonances from anomeric protons of the terminal mannopyranosyl groups. While this is straightforward for disaccharides **2** and **4**, notably, in trisaccharide **8**, the anomeric ^{1}H NMR chemical shifts at the α(1 → 3)-linkage are degenerate for **2**
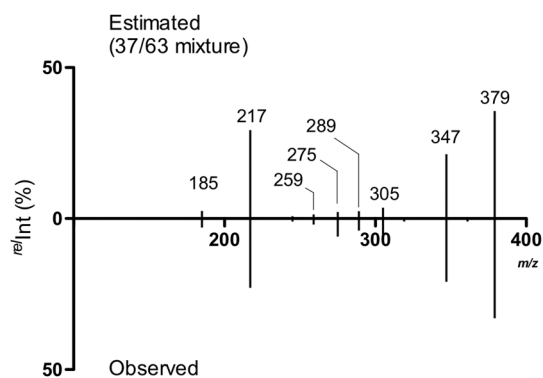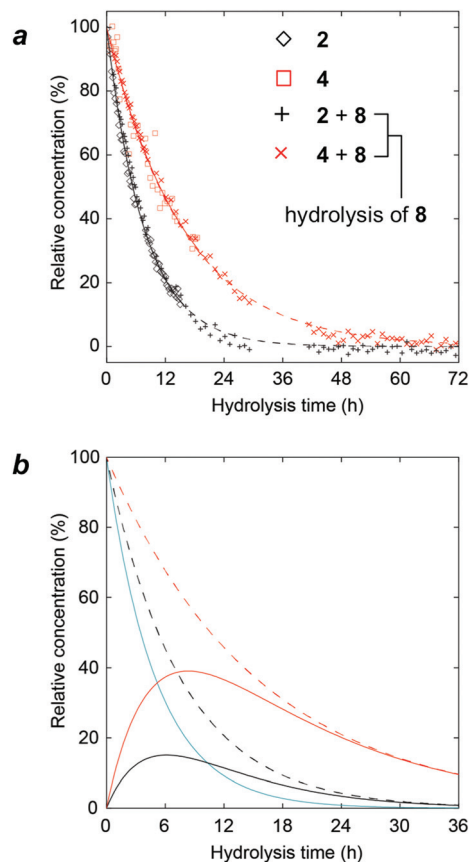

Fig. 9 NMR analysis of hydrolysis reactions. (a) Time-course for acid hydrolysis (1 M TFA in D₂O at 70 °C) of the 3,6-disubstituted trisaccharide **8**, the constituent disaccharides **2** and **4**, α-(1 → 3)- and α-(1 → 6)-linked, respectively, analyzed using ^{1}H NMR spectroscopy with (◇) **2**, (□) **4**, (+) **2** and **8**, (×) **4** and **8**, whose fitted data are represented by solid black, solid red, dashed black, and dashed red lines, respectively; (b) calculated time-course for the acid hydrolysis of the 3,6-disubstituted trisaccharide **8** (cyan). The hydrolysis intermediates, *i.e.*, disaccharides **2** and **4**, are shown as black and red lines, respectively. The sum of **2** and **8** is shown by the dashed black line and the dashed red line corresponds to the sum of **4** and **8**.

Fig. 8 Estimated MS/MS spectrum of the ion mixture of constituting disaccharide ions and the observed spectrum.

and **8** and this is also the case for the α(1 → 6)-linkages in compounds **4** and **8**. This degeneracy indicates that in the trisaccharide, the hydrolysis of **2** and **8** is monitored at the α(1 → 3)-linkage and in the same way, the hydrolysis reaction for the α(1 → 6)-linkage is followed, but not differentiated, for compounds **4** and **8**. In the disaccharides, the α-ᴅ-Man*p* group linked to *O*3 showed $t_{1/2}$ = 5.3 h, whereas when linked to *O*6, $t_{1/2}$ = 10.9 h. When these data were compared to the apparent hydrolysis rates in the trisaccharide, $t_{1/2}$ = 5.4 h and $t_{1/2}$ = 10.7 h, respectively, it became evident that the reactivity in the trisaccharide is similar to that of its constituent disaccharides. The experimentally determined half-lives were used to calculate the evolution of the composition of the trisaccharide and the two disaccharides over the course of the hydrolysis reaction of the trisaccharide (Fig. 9b). The hydrolysis of **8** (cyan line in Fig. 9b) is at its initial stage foremost owing to the cleavage of the α(1 → 3)-linkage resulting in the rapid formation of disac-

This journal is © The Royal Society of Chemistry 2018

Org. Biomol. Chem., 2018, **16**, 228–238 | 233

charide **4** (red line in Fig. 9b). During the later course of the reaction, consequently, its α(1 → 6)-linkage is cleaved, which can be observed from the significantly higher concentration of **4** compared to that of **2** (red and black lines in Fig. 9b, respectively).

The fact that hydrolysis at the α(1 → 3)-linkage occurred twice as fast as that at the α(1 → 6)-linkage for the mannose-containing oligosaccharides when using 1 M trifluoroacetic acid (TFA) at 70 °C is consistent with the previous results of hydrolysis rates for α(1 → 3)-linked nigerose, which was hydrolyzed 4.5 times faster in 0.1 N hydrochloric acid at 80 °C than α(1 → 6)-linked isomaltose; furthermore, at 99.5 °C, it was hydrolyzed 3 times faster.[30] Notably, the hydrolysis rates at the α-D-Man*p*-linkages mirrored the stability of the mannose oligosaccharides when subjected to CID and the propensity to fragment as detected using MS. Although our result may be seen as partially contradictory to the hydrolysis results of *S. cerevisiae* mannan where the order of mannose release is not precisely controlled, the presence of branching mannoside such as mannosyl residues with the oligosaccharide attached to both 2- and 6-positions might be highly reactive due to steric factors.[31] Thus the observed phenomena in this investigation cannot be directly applied to the hydrolysis of higher glycan structures.

Conclusions

A series of synthetic disaccharides and trisaccharides consisting of α-linked mannopyranoside were used to investigate gas-phase CID reactions and acid hydrolyses. Analyses data of all the possible linkage-isomers of α-mannosyl disaccharides were used in the analyses of trisaccharides. As the dissociation reactions of ions of trisaccharides produce their partial structures including disaccharide equivalent ions called Y-ions, it was confirmed that individual trisaccharides contained the corresponding disaccharides. This indicates that an array of low-level glycans is powerful in investigation higher glycan structures. The linkage isomers of these constituting disaccharides could be discriminated using low-energy CID experiments where the patterns of a series of produced product ions were different. Individual structures could also be differentiated based on ERMS. The analysis of linear trisaccharides revealed that the order of dissociation of the linkage isomers was the same as that of disaccharides when a common mannosyl cleavage was used as the internal energy reference. Furthermore, a 3- and 6-branched trisaccharide showed a distinctive dissociation pattern producing a lower number of product ions. As the branched compound produced two constituting disaccharide ions, the estimation of their population in the ion mixture was possible using the individual spectra of the disaccharides. Furthermore, the reaction progress of the hydrolytic glycosyl cleavages of 3- and 6-linked disaccharides and the branched trisaccharide was monitored using NMR, and compared with gas-phase dissociation reactions. The results indicated that the cleavage-reaction rates mirrored those observed in CID experi-

ments. The results obtained herein may provide information for elucidating α-glycosidically linked mannosyl structures and may, in the future, be extended to other sugar residues with *gluco-* or *galacto-*configurations and β-linked oligosaccharides, some of which have been studied using the ERMS technique.[32]

Experimental

General

The oligosaccharides methyl α-D-mannopyranosyl-(1 → 2)-α-D-mannopyranoside (**1**), methyl α-D-mannopyranosyl-(1 → 3)-α-D-mannopyranoside (**2**), methyl α-D-mannopyranosyl-(1 → 6)-α-D-mannopyranoside (**4**), methyl α-D-mannopyranosyl-(1 → 6)-α-D-[6-¹³C]mannopyranoside (**4c**), methyl α-D-mannopyranosyl-(1 → 2)-α-D-mannopyranosyl-(1 → 2)-α-D-mannopyranoside (**5**), methyl α-D-mannopyranosyl-(1 → 2)-α-D-mannopyranosyl-(1 → 3)-α-D-mannopyranoside (**6**) were available from previous studies[33–35] and methyl α-D-mannopyranosyl-(1 → 3)[α-D-mannopyranosyl-(1 → 6)]-α-D-mannopyranoside (**8**) was purchased from Carbosynth, Compton, UK.

Synthesis

General. All reagents were used as delivered. Column chromatography was performed manually on silica gel with a pore size of 60 Å or by using a Biotage Isolera flash purification system with KP-Sil snap chromatography cartridges. TLC was carried out on silica gel 60 F$_{254}$ (20 × 20 cm, 0.2 mm thickness), and monitored with either UV light 254 nm or sulfuric acid 8%. NMR spectra for characterization were recorded at 27 °C on spectrometers operating at a ¹H frequency of 400 or 500 MHz, except for compounds **3** and **7** that were recorded at 24 °C and 25 °C, respectively. The NMR chemical shifts are reported in ppm and for ¹H referenced to TMS, sodium 3-trimethylsilyl-(2,2,3,3-²H$_4$)-propanoate (TSP), both set to 0 ppm, or the residual CHCl$_3$ solvent peak at 7.26 ppm as an internal standard; for ¹³C the chemical shifts were referenced to 1,4-dioxane in D$_2$O, 67.40 ppm, using an external standard or internally to the CDCl$_3$ solvent signal at 77.16 ppm. For compounds **3** and **7** ¹H chemical shifts and J_{HH} coupling constants were refined from 1D ¹H NMR spectra using a NMR spin simulation methodology.[36] High resolution mass spectra were recorded on a Bruker Daltonics micrOTOF spectrometer in positive mode.

Methyl 2,3,4,6-tetra-*O*-benzoyl-α-D-mannopyranosyl-(1 → 4)-2,3,6-tri-*O*-benzyl-α-D-mannopyranoside (11). Methyl 2,3,6-tri-*O*-benzyl-α-D-mannopyranoside (**9**)[37,38] (62.3 mg, 134.1 μmol) and ethyl 2,3,4,6-tetra-*O*-benzoyl-1-thio-α-D-mannopyranoside (**10**)[39–41] (128.9 mg, 201.2 μmol) were dissolved in DCM (1 mL) under an argon atmosphere and stirred with 4 Å molecular sieves. After cooling the solution to −50 °C, NIS (60.0 mg, 268.2 μmol) was added followed by a catalytic amount of AgOTf. The temperature was allowed to rise to −30 °C over 45 min after which TLC indicated completion. After quenching with Et$_3$N (a few drops), the mixture was filtered through Celite and the solvent removed under reduced pressure. Purification

234 | *Org. Biomol. Chem.*, 2018, **16**, 228–238

This journal is © The Royal Society of Chemistry 2018

using silica column chromatography (gradient, toluene → toluene/EtOAc: 20/1) yielded title compound **11** (117 μg, 0.112 μmol) in 84% yield. ^{13}C-NMR (CDCl$_3$): δ = 55.1 (OMe), 62.9–80.2 (10 C2–C6, 3 BnCH$_2$), 98.9, 99.4 (2 anomeric), 127.6–138.4 (42 aromatic), 165.0–166.2 (4 CO). ^{1}H-NMR (CDCl$_3$): δ = 3.41 (3H, s, OMe), 3.75 (1H, dd, J = 1.9, 3.1 Hz, H2), 3.82–3.91 (2H, m, H6), 3.92 (1H, m, H5), 4.01 (1H, dd, J = 3.1, 9.2 Hz, H3), 4.22 (1H, dd, J = 3.8, 12.2 Hz, H6′$_{pro-R}$), 4.27 (1H, dd, J = 9.2, 9.2 Hz, H4), 4.29 (1H, ddd, J = 2.5, 3.8, 10.0 Hz, H5′), 4.40 (1H, dd, J = 2.5, 12.2 Hz, H6′$_{pro-S}$), 4.56–4.71 (6 H, m, PhCH$_2$), 4.79 (1H, d, J = 1.9 Hz, H1), 5.64 (1H, d, J = 1.9 Hz, H1′), 5.79 (1H, dd, J = 1.9, 3.2 Hz, H2′), 5.82 (1H, dd, J = 3.2, 10.0 Hz, H3′), 6.02 (1H, dd, J = 10.0, 10.0 Hz, H4′), 7.02–8.13 (35H, aromatic). ESI-MS: m/z [M + Na]$^+$ calc. for C$_{62}$H$_{58}$NaO$_{15}$ 1065.3668, found 1065.3681.

Methyl α-D-mannopyranosyl-(1 → 4)-α-D-mannopyranoside (3). Methyl 2,3,4,6-tetra-O-benzoyl-α-D-mannopyranosyl-(1 → 4)-2,3,6-tri-O-benzyl-α-D-mannopyranoside (**11**) (70.8 mg, 67.9 μmol) was dissolved in an equal mixture of EtOAc and EtOH (5 mL) and a catalytic amount of Pd(OH)$_2$ was added followed by a drop of HCl (37% aq.). The mixture was placed under a hydrogen atmosphere (100 psi) and stirred for 30 hours. After filtering through Celite and rinsing with EtOH, the solvent was removed *in vacuo*. The resulting debenzylated material was dissolved in MeOH (10 mL) and NaOMe was added until the solution was slightly basic (pH ≈ 9). After stirring for 24 hours, Dowex-50 (H$^+$-form) was added followed by filtration, rinsing with MeOH and evaporation of the solvent. The resulting crude product was purified on a C18 reverse phase cartridge, eluting with H$_2$O. After lyophilization, the material was purified using gel-permeation chromatography on an ÄKTApurifier equipped with a Superdex™ 30 column, prep. grade gel (GE Healthcare, Uppsala, Sweden) using water containing 1% *n*-butanol as the eluent. The title compound **3** (13.4 mg, 37.6 μmol) was obtained in 55% yield. ^{13}C-NMR (D$_2$O): δ = 55.5 (OMe), 61.7 (C6′), 61.9 (C6), 67.4 (C4′), 71.1 (C2′), 71.1 (C3′), 71.2 (C2), 71.9 (C3), 71.8 (C5), 74.5 (C5′), 75.1 (C4), 101.5 (C1, $^1J_{C,H}$ = 171 Hz), 102.3 (C1′, $^1J_{C,H}$ = 172 Hz). ^{1}H-NMR (D$_2$O): δ = 3.42 (3H, s, OMe), 3.68 (1H, dd, $^3J_{H4′,H5′}$ = 10.0 Hz, H4′), 3.68 (1H, ddd, $^3J_{H5′,H6′pro-R}$ = 5.7 Hz; $^3J_{H5′,H6′pro-S}$ = 2.1 Hz, H5′), 3.70 (1H, dd, $^3J_{H5,H6pro-R}$ = 5.8 Hz; $^3J_{H5,H6pro-S}$ = 2.1, H5), 3.77 (1H, dd, $^2J_{H6′pro-R,H6′pro-S}$ = −12.3 Hz, H6′$_{pro-R}$), 3.81 (1H, dd, $^3J_{H3′,H4′}$ = 9.4 Hz, H3′), 3.81 (1H, dd, $^2J_{H6pro-R,H6pro-S}$ = −12.1 Hz, H6$_{pro-R}$), 3.82 (1H, dd, $^3J_{H4,H5}$ = 10.0 Hz, H4), 3.90 (1H, dd, H6′$_{pro-S}$), 3.91 (1H, dd, $^3J_{H2,H3}$ = 3.6 Hz, H2), 3.91 (1H, dd, H6$_{pro-S}$), 3.92 (1H, dd, $^3J_{H3,H4}$ = 9.1 Hz, H3), 4.06 (1H, dd, $^3J_{H2′,H3′}$ = 3.3 Hz, H2′), 4.78 (1H, d, $^3J_{H1,H2}$ = 1.5 Hz, H1), 5.25 (1H, d, $^3J_{H1′,H2′}$ = 1.9 Hz, H1′). ESI-MS: m/z [M + Na]$^+$ calc. for C$_{13}$H$_{24}$NaO$_{11}$ 379.1211, found 379.1213.

Methyl 3,4,6-tri-O-benzyl-α-D-mannopyranosyl-(1 → 6)-2,3,4-tri-O-benzyl-α-D-mannopyranoside (14). A solution of methyl 2,3,4-tri-O-benzyl-α-D-mannopyranoside (**12**)[37] (538 mg, 1.16 mmol) and ethyl 2-O-acetyl-3,4,6-tri-O-benzyl-1-thio-α-D-mannopyranoside (**13**)[42–44] (778 mg, 1.50 mmol) was stirred in DCM (15 mL) with molecular sieves at −30 °C. NIS (311 mg, 1.38) and AgOTf (spatula tip) were added. After 15 minutes,

the reaction mixture turned deep red and was quenched with Et$_3$N. After filtering through Celite, diluting with DCM and washing with sat. Na$_2$S$_2$O$_3$ (aq.) and brine, the organic phase was dried with MgSO$_4$ and the solvent was removed under reduced pressure. The resulting brown oil was applied to a silica column (6 : 1 toluene : EtOAc) giving methyl 2-O-acetyl-3,4,6-tri-O-benzyl-α-D-mannopyranosyl-(1 → 6)-2,3,4-tri-O-benzyl-α-D-mannopyranoside in 58% yield (632 mg, 0.673 mmol). This compound (629 mg, 0.670 mmol) was then dissolved in MeOH and NaOMe was added until pH ≈ 9. After 21 hours, Dowex-50 (H$^+$-form) was added prior to filtration and removal of the solvent under reduced pressure. After purification on silica gel (toluene/EtOAc: 7/3) product **14**[45] was obtained in 53% yield over two steps (547 mg, 0.610 mmol). ^{13}C-NMR (CDCl$_3$): δ = 54.74 (OMe), 66.4–80.2 (10 C2–C6, 6 PhCH$_2$), 98.9 (C1, $^1J_{C1,H1}$ = 169.8 Hz), 99.7 (C1′, $^1J_{C1′,H1′}$ = 170.9 Hz), 127.6–128.5 (30 aromatic), 137.9–138.6 (6 i-Bn). ^{1}H-NMR (CDCl$_3$): δ = 2.32 (1H, d, J = 2.9 Hz, HO2′), 3.26 (1H, s, 3H, OMe), 3.57–4.93 (27H, H1, H2–H6, H2′–H6′, 6 PhCH2), 5.07 (1H, d, J = 1.8 Hz, H1′), 7.13–7.39 (30H, aromatic). ESI-MS: m/z [M + Na]$^+$ calc. for C$_{55}$H$_{60}$NaO$_{11}$ 919.4028, found 919.4029.

Methyl 2,3,4,6-tetra-O-benzoyl-α-D-mannopyranosyl-(1 → 2)-3,4,6-tri-O-benzyl-α-D-mannopyranosyl-(1 → 6)-2,3,4-tri-O-benzyl-α-D-mannopyranoside (15). A solution of methyl 3,4,6-tri-O-benzyl-α-D-mannopyranosyl-(1 → 6)-2,3,4-tri-O-benzyl-α-D-mannopyranoside (**14**) (43.3 mg, 48.2 μmol) and ethyl 2,3,4,6-tetra-O-benzoyl-1-thio-α-D-mannopyranoside (**10**) (38.7 mg, 60.4 μmol) in DCM (1 mL) was stirred with molecular sieves under an argon atmosphere while being cooled to −30 °C. NIS (31.6 mg, 140.4 μmol) was added followed by a spatula tip of AgOTf. After 30 min, the color had turned to dark red and Na$_2$S$_2$O$_3$ (sat. aq.) was added. The solution was filtered through a plug of Celite and extracted thrice with toluene. The combined organic phase was washed with water, followed by brine, dried with MgSO$_4$ and concentrated under reduced pressure. The crude product was purified on a column of silica (gradient, toluene → toluene/EtOAc: 13/1) giving product **15** in 67% yield (48.3 mg, 32.2 μmol). ^{13}C-NMR (CDCl$_3$): δ = 54.8 (OMe), 62.9–80.3 (15 C2–6, 6 PhCH$_2$), 98.9–99.8 (3 anomeric), 127.5–138.8 (60 aromatic), 165.2–166.3 (4 CO). ^{1}H-NMR (CDCl$_3$): δ = 3.26 (3H, s, OMe), 3.59–4.76 (25H, 15 H2–6, 10 PhCH$_2$), 4.81–5.24 (3H, 3 × d, J = 1.8, 1.9, 1.9 Hz, H1, H1′, H1″), 4.88 (1H, d, J = 11.1, PhCH$_2$), 4.92 (1H, d, J = 11.0 Hz, PhCH$_2$), 5.93 (1H, dd, J = 1.9, 3.2 Hz, H2″), 5.99 (1H, dd, J = 3.2, 10.1 Hz, H3″), 6.20 (1H, dd, J = 10.1, 10.1 Hz, H4″), 7.04–8.17 (50H, aromatic). ESI-MS: m/z [M + Na]$^+$ calc. for C$_{89}$H$_{86}$NaO$_{20}$ 1497.5605, found 1497.5589.

Methyl α-D-mannopyranosyl-(1 → 2)-α-D-mannopyranosyl-(1 → 6)-α-D-mannopyranoside (7). Methyl 2,3,4,6-tetra-O-benzoyl-α-D-mannopyranosyl-(1 → 2)-3,4,6-tri-O-benzyl-α-D-mannopyranosyl-(1 → 6)-2,3,4-tri-O-benzyl-α-D-mannopyranoside (**15**) (114.8 mg, 77.7 μmol) was dissolved in EtOAc : EtOH (1 : 1, 5 mL) and Pd(OH)$_2$/C (spatula tip) as well as a drop of HCl were added (37% aq.). The mixture was stirred under H$_2$ (110 psi) overnight before being filtered through Celite and the solvent being evaporated. The residue was dissolved in MeOH

Paper

and NaOMe was added until pH ≈ 9 before stirring overnight. Dowex-50 (H⁺-form) was added and stirred for a few minutes before filtering and removing the solvent under reduced pressure. The crude material was applied to a C-18 reversed-phase cartridge eluting with H_2O and lyophilized before being purified by gel-permeation chromatography on an ÄKTApurifier equipped with a Superdex™ 30 column, prep. grade gel (GE Healthcare, Uppsala, Sweden), using water containing 1% *n*-butanol as the eluent. Compound **7** was obtained in 31% yield (12.7 mg, 24.4 μmol). ¹³C-NMR (D₂O): δ = 55.46 (OMe), 61.60 (C6′), 61.79 (C6″), 66.43 (C6), 67.19 (C4), 67.54 (C4″), 67.59 (C4′), 70.55 (C2), 70.63 (C2″), 70.91 (C3′), 70.99 (C3″), 71.37 (C5), 71.42 (C3), 73.43 (C5′), 73.91 (C5″), 79.36 (C2′), 98.65 (C1′, $^1J_{C′,H′}$ = 172 Hz), 101.71 ($^1J_{C,H}$ = 171 Hz, C1), 103.02 ($^1J_{C″,H″}$ = 171 Hz, C1″). ¹H-NMR (D₂O): δ = 3.40 (3H, s, OMe), 3.62 (1H, dd, $^3J_{H4″,H5″}$ = 10.0 Hz, H4″), 3.69 (1H, ddd, $^3J_{H5′,H6′pro-R}$ = 5.7 Hz; $^3J_{H5′,H6′pro-S}$ = 2.0 Hz, H5′), 3.69 (1H, dd, $^3J_{H4′,H5′}$ = 9.3 Hz, H4′), 3.72 (1H, dd, $^3J_{H4,H5}$ = 9.9 Hz, H4), 3.73 (1H, dd, $^2J_{H6″pro-R,H6″pro-S}$ = −12.3 Hz, H6″pro-R), 3.74 (1H, dd, $^3J_{H3,H4}$ = 9.4 Hz, H3), 3.74 (1H, ddd, $^3J_{H5,H6pro-R}$ = 4.7 Hz; $^3J_{H5,H6pro-S}$ = 1.6 Hz, H5), 3.75 (1H, dd, $^2J_{H6pro-R,H6pro-S}$ = −11.7 Hz, H6pro-S), 3.76 (1H, dd, $^2J_{H6′pro-R,H6′pro-S}$ = −12.2 Hz, H6′pro-R), 3.77 (1H, ddd, $^3J_{H5″,H6″pro-R}$ = 6.6 Hz; $^3J_{H5″,H6″pro-S}$ = 2.2 Hz, H5″), 3.84 (1H, dd, $^3J_{H3″,H4″}$ = 9.7 Hz, H3″), 3.89 (1H, dd, H6″pro-S), 3.89 (1H, dd, H6′pro-S), 3.93 (1H, dd, $^3J_{H2,H3}$ = 3.4 Hz, H2), 3.95 (1H, dd, $^3J_{H3′,H4′}$ = 9.6 Hz, H3′), 3.96 (1H, dd, H6pro-R), 4.01 (1H, dd, $^3J_{H2′,H3′}$ = 3.4 Hz, H2′), 4.07 (1H, dd, $^3J_{H2″,H3″}$ = 3.4 Hz, H2″), 4.74 (1H, d, $^3J_{H1,H2}$ = 1.7 Hz, H1), 5.02 (1H, d, $^3J_{H1″,H2″}$ = 1.8 Hz, H1″), 5.14 (1H, d, $^3J_{H1′,H2′}$ = 1.8 Hz, H1′). ESI-MS: *m/z* [M + Na]⁺ calc. for $C_{19}H_{34}NaO_{16}$ 541.1739, found 541.1731.

Methyl α-D-mannopyranosyl-(1 → 2)-α-D-mannopyranosyl-(1 → 6)-α-D-[6-¹³C]mannopyranoside (7c). Starting from 2,3,4-tri-O-benzyl-α-D-[6-¹³C]mannopyranoside[34] (**12c**) (120 mg, 257 μmol) and using the same procedure as that for the unlabeled compound, methyl 3,4,6-tri-O-benzyl-α-D-mannopyranosyl-(1 → 6)-2,3,4-tri-O-benzyl-α-D-[6-¹³C]mannopyranoside (**14c**) was obtained in 62% yield (143 mg, 159 μmol). ESI-MS: *m/z* [M + Na]⁺ calc. for $C_{54}{}^{13}CH_{60}NaO_{11}$ 920.4061, found 920.4067. A solution of methyl 3,4,6-tri-O-benzyl-α-D-mannopyranosyl-(1 → 6)-2,3,4-tri-O-benzyl-α-D-[6-¹³C]mannopyranoside (**14c**) (134 mg, 149 μmol) and ethyl 2,3,4,6-tetra-O-benzoyl-1-thio-α-D-mannopyranoside (**10**) (120 mg, 184 μmol) in DCM (2 mL) was stirred with molecular sieves under an argon atmosphere while being cooled to −30 °C. NIS (67.2 mg, 300 μmol) was added followed by a spatula tip of AgOTf. After 50 min, the color had turned dark red and sat. Na₂S₂O₃ (aq.) was added. The solution was extracted three times with toluene, the combined organic phase was washed with brine, dried over MgSO₄ and concentrated under reduced pressure. The crude product was purified on a column of silica (toluene → toluene/EtOAc: 13/1) followed by a second column of silica (pentane → pentane/EtOAc: 3/1) yielding methyl 2,3,4,6-tetra-O-benzoyl-α-D-mannopyranosyl-(1 → 2)-3,4,6-tri-O-benzyl-α-D-mannopyranosyl-(1 → 6)-2,3,4-tri-O-benzyl-α-D-[6-¹³C]mannopyranoside (**15c**) in 45% yield (99.3 mg, 67.2 μmol). ESI-MS:

m/z [M + Na]⁺ calc. for $C_{88}{}^{13}CH_{86}NaO_{20}$ 1498.5638, found 1498.5584.

Following the same procedure as that for the unlabeled compound, methyl 2,3,4,6-tetra-O-benzoyl-α-D-mannopyranosyl-(1 → 2)-3,4,6-tri-O-benzyl-α-D-mannopyranosyl-(1 → 6)-2,3,4-tri-O-benzyl-α-D-[6-¹³C]mannopyranoside (**15c**) (120.8 mg, 81.8 μmol) gave the title compound **7c** in 63% yield (26.7 mg, 51.3 μmol). ESI-MS: *m/z* [M + Na]⁺ calc. for $C_{18}{}^{13}CH_{34}NaO_{16}$ 542.1773, found 542.1771.

Mass spectrometric analysis of glycans

Instrumentation and data collection. Samples of disaccharides were analyzed using a quadrupole ion trap mass spectrometer (QIT-MS) coupled with an electrospray interface (Amazon ETD) (Bruker Daltonics, GmbH, Bremen, Germany). Samples dissolved in MeOH (*ca.* 0.1 μmol mL⁻¹) were introduced into the ion source *via* infusion (flow rate, 120 μL h⁻¹). The parameters for the analysis were: (1) dry temperature: 200 °C, (2) nebulizer gas (N₂): 10 psi, (3) dry gas (N₂): 4.0 L min⁻¹, (4) scan range: *m/z* 50–750, (5) compound stability: 100%, (6) ion charge control, on/target, 200 000, (7) maximum acquisition time: 200 ms, (8) average: 5 spectra, and (9) polarity, positive. In our MSⁿ experiments, the end cap rf amplitude was raised by 0.02 V increments until the precursor ion could no longer be detected. Only the end cap rf amplitude was controlled during the CID experiment. The He pressure was 4.86 × 10⁻⁶ mbar and the CID time was 40 ms. Averages of 15 spectra were used for CID experiments. Isotopic peaks with [I^i + 1] and [I^i + 2], where I^n indicates a fragment ion, were included in the calculations. For the isolation of a product ion, *m/z* ± 2 (*w* = 2) were isolated and subjected to the CID experiments to include isotopes. Standard MS/MS spectra are the extracts of this ERMS at a designated amplitude.

Data manipulation. In order to obtain graphs of the ERMS, the following equations were used. When an ion "I^P" produces a series of product ions, I^1, I^2, I^3,... I^i, the relative ion currents for individual ions were defined by the equation,

$$^{\mathrm{rel}}C = \frac{C^{I^i}}{C^{I^P} + \sum_{i=1}^{n} C^{I^i}} \times 100 \quad (1)$$

where $^{\mathrm{rel}}C$ indicates the ion current of a given ion among the observed ions in percentage, C^{I^i} is the observed ion current in focus, and C^{I^P} is the ion current of a precursor ion. The calculations were performed using a program we developed with Excel (Excel 2000 (Microsoft Co.)), which was based on the DSUM function and programmed to choose a range of isotopes (*w*) to be taken into consideration (*w* = 2 in the experiments).

Hydrolysis of oligosaccharides

Acid hydrolysis reactions were carried out in 5 mm NMR tubes containing compound **2** (1.0 mg), **4** (1.0 mg) or **8** (1.5 mg) using 1 M TFA in D₂O (0.5–0.6 mL) at 343.15 K. The reaction progress was monitored by one-dimensional ¹H NMR spectroscopy at 500 MHz analyzing for the disappearance of perti-

nent anomeric proton resonances; the approximate degeneracy of the anomeric ^{1}H chemical shifts in **8** *vs.* **2** or **4** was confirmed by NMR chemical shift predictions using the CASPER program.[46]

Conflicts of interest

There are no conflicts to declare.

Acknowledgements

Notes and references

1 Y. Kanie and O. Kanie, *Biol. Chem. Compos.*, 2017, **5**, 3, DOI: 10.7243/2052-9341-5-3.

2 S. Daikoku, T. Ako, R. Kato, I. Ohtsuka and O. Kanie, *J. Am. Soc. Mass Spectrom.*, 2007, **18**, 1873–1879.

3 S. Daikoku, T. Ako, A. Kurimoto and O. Kanie, *J. Mass Spectrom.*, 2007, **42**, 714–723.

4 D. J. Harvey, A. H. Merry, L. Royle, M. P. Campbell, R. A. Dwek and P. M. Rudd, *Proteomics*, 2009, **9**, 3796–3801.

5 A. Varki, R. D. Cummings, M. Aebi, N. H. Packer, P. H. Seeberger, J. D. Esko, P. Stanley, G. Hart, A. Darvill, T. Kinoshita, J. J. Prestegard, R. L. Schnaar, H. H. Freeze, J. D. Marth, C. R. Bertozzi, M. E. Etzler, M. Frank, J. F. Vliegenthart, T. Lütteke, S. Perez, E. Bolton, P. Rudd, J. Paulson, M. Kanehisa, P. Toukach, K. F. Aoki-Kinoshita, A. Dell, H. Narimatsu, W. York, N. Taniguchi and S. Kornfeld, *Glycobiology*, 2015, **25**, 1323–1324.

6 *Symbol Nomenclature for Glycans (SNFG), Essentials of Glycobiology*, ed. A. Varki, R. D. Cummings, J. D. Esko, P. Stanley, G. Hart, M. Aebi, A. Darvill, T. Kinoshita, N. H. Packer, J. H. Prestegard, R. L. Schnaar and P. H. Seeberger, Cold Spring Harbor (NY): Cold Spring Harbor Laboratory Press, 3rd edn, 2015, Appendix 1B.

7 http://www.functionalglycomics.org/static/consortium/Nomenclature.shtml.

8 A. Helenius and M. Aebi, *Annu. Rev. Biochem.*, 2004, **73**, 1019–1049.

9 S. Dejgaard, J. Nicolay, M. Taheri, D. Y. Thomas and J. J. M. Bergeron, *Curr. Issues Mol. Biol.*, 2004, **6**, 29–42.

10 S.-H. Son, A. Seko, S. Daikoku, K. Fujikawa, K. Suzuki, Y. Ito and O. Kanie, *ChemBioChem*, 2016, **17**, 630–639.

11 K. J. Dooresa, C. Bonomelli, D. J. Harvey, S. Vasiljevic, R. A. Dwek, D. R. Burtona, M. Crispin and C. N. Scanlan, *Proc. Natl. Acad. Sci. U. S. A.*, 2010, **107**, 13800–13805.

12 P. M. Rudd, M. R. Wormald and R. A. Dwek, *Trends Biotechnol.*, 2004, **22**, 524–530.

13 S. J. Lee, S. Evers, D. Roeder, A. F. Parlow, J. Risteli, L. Risteli, Y. C. Lee, T. Feizi, H. Langen and M. C. Nussenzweig, *Science*, 2002, **295**, 1898–1901.

14 S. J. Van Dyken and R. M. Locksley, *Immunol. Cell Biol.*, 2007, **85**, 572–574.

15 G. A. Rabinovich and D. O. Croci, *Immunity*, 2012, **36**, 322–335.

16 M. G. Paulick and C. R. Bertozzi, *Biochemistry*, 2008, **47**, 6991–7000.

17 P. Orlean, Cell Wall, *Genetics*, 2012, **192**, 775–818.

18 F. Cuskin, E. C. Lowe, M. J. Temple, Y. Zhu, E. A. Cameron, N. A. Pudlo, N. T. Porter, K. Urs, A. J. Thompson, A. Cartmell, A. Rogowski, B. S. Hamilton, R. Chen, T. J. Tolbert, K. Piens, D. Bracke, W. Vervecken, Z. Hakki, G. Speciale, J. L. Munōz-Munōz, A. Day, M. J. Pen, R. McLean, M. D. Suits, A. B. Boraston, T. Atherly, C. J. Ziemer, S. J. Williams, G. J. Davies, D. W. Abbott, E. C. Martens and H. J. Gilbert, *Nature*, 2015, **517**, 165–169.

19 S. K. Maitra and C. E. Ballou, *J. Biol. Chem.*, 1977, **252**, 2459–2469.

20 R. Lain, K. M. Pamidimukkala, A. D. French, R. W. Hall, S. Abbas, R. Jain and K. L. Matta, *J. Am. Chem. Soc.*, 1988, **110**, 6931–6939.

21 J. Hofmann, H. S. Hahm, P. H. Seeberger and K. Pagel, *Nature*, 2015, **526**, 241–244.

22 S. H. Khan, C. F. Piskorz and K. L. Matta, *J. Carbohydr. Chem.*, 1994, **13**, 1025–1035.

23 D. Kotsyubynskyy, M. Zerbetto, M. Soltesova, O. Engström, R. Pendrill, J. Kowalewski, G. Widmalm and A. Polimeno, *J. Phys. Chem. B*, 2012, **116**, 14541–14555.

24 S. Daikoku, A. Kurimoto, S. Mutsuga, T. Ako, T. Kanemitsu, Y. Shioiri, A. Ohtake, R. Kato, C. Saotome, I. Ohtsuka, S. i. Koroghi, S. K. Sarkar, A. Tobe, S. Adachi, K. Suzuki and O. Kanie, *Carbohydr. Res.*, 2009, **344**, 384–394.

25 A. Kurimoto, S. Daikoku, S. Mutsuga and O. Kanie, *Anal. Chem.*, 2006, **78**, 3461–3466.

26 B. Domon and C. E. Costello, *Glycoconjugate J.*, 1988, **5**, 397–409.

27 A. Kameyama, N. Kikuchi, S. Nakaya, H. Ito, T. Sato, T. Shikanai, Y. Takahashi, K. Takahashi and H. Narimatsu, *Anal. Chem.*, 2005, **77**, 4719–4725.

28 H. Ito, Y. Takegawa, K. Deguchi, S. Nagai, H. Nakagawa, Y. Shinohara and S.-I. Nishimura, *Rapid Commun. Mass Spectrom.*, 2006, **20**, 3557–3565.

29 R. Schoenheimer and D. Rittenberg, *Science*, 1938, **87**, 221–226.

30 M. L. Wolfrom, A. Thompson and C. E. Timberlake, *Cereal Chem.*, 1963, **40**, 82–86.

31 K. Ogawa, J.-I. Nishikori, T. Ino and K. Matsuda, *Biosci., Biotechnol., Biochem.*, 1994, **58**, 560–562.

32 S. Daikoku, G. Widmalm and O. Kanie, *Rapid Commun. Mass Spectrom.*, 2009, **23**, 3713–3719.

33 P.-E. Jansson and G. Widmalm, *J. Chem. Soc., Perkin Trans. 2*, 1992, 1085–1090.

34 U. Olsson, E. Saewen, R. Stenutz and G. Widmalm, *Chem. – Eur. J.*, 2009, **15**, 8886–8894.

This journal is © The Royal Society of Chemistry 2018

Org. Biomol. Chem., 2018, **16**, 228–238 | 237

35 C. Johannessen, R. Pendrill, G. Widmalm, L. Hecht and L. D. Barron, *Angew. Chem.*, 2011, **123**, 5461–5463, (*Angew. Chem. Int. Ed.*, 2011, **50**, 5349–5351).

36 R. Laatikainen, M. Niemitz, U. Weber, J. Sundelin, T. Hassinen and J. Vepsäläinen, *J. Magn. Reson., Ser. A*, 1996, **120**, 1–10.

37 C. Bernlind, S. Oscarson and G. Widmalm, *Carbohydr. Res.*, 1994, **263**, 173–180.

38 S. D. Debenham and E. J. Toone, *Tetrahedron: Asymmetry*, 2000, **11**, 385–387.

39 P. J. Garegg, J.-L. Maloisel and S. Oscarson, *Synthesis*, 1995, 409–414.

40 S. Sarbajna and N. Roy, *Indian J. Chem., Sect. B: Org. Chem. Incl. Med. Chem.*, 1998, **37**, 252–256.

41 D. Sail and P. Kovác, *Carbohydr. Res.*, 2012, **357**, 47–52.

42 T. Peters, *Liebigs Ann. Chem.*, 1991, **1991**, 135–141.

43 R. K. Jain, X.-G. Liu, S. R. Oruganti, E. V. Chandrasekaran and K. L. Matta, *Carbohydr. Res.*, 1995, **271**, 185–196.

44 F. Barresi and O. Hindsgaul, *Can. J. Chem.*, 1994, **72**, 1447–1465.

45 V. K. Srivastava and C. Schurtch, *J. Org. Chem.*, 1981, **46**, 1121–1126.

46 M. Lundborg and G. Widmalm, *Anal. Chem.*, 2011, **83**, 1514–1517.